

酰肼氧钒(V)配合物的合成、结构及其抑制幽门螺旋杆菌脲酶研究

张吉才 李海华 献冬梅 张 梅 甄苗苗 赵 月 由忠录*

(辽宁师范大学化学化工学院, 大连 116029)

摘要: 本文合成了 2 个新的结构类似的酰肼氧钒(V)配合物, $[\text{VOL}(\text{OCH}_3)(\text{CH}_3\text{OH})](\text{L}=\text{L}^1=2\text{-氯-}N'-(5\text{-氯-2-羟基苯亚甲基})\text{苯甲酰肼}(\mathbf{1}); \text{L}=\text{L}^2=2\text{-氯-}N'-(2\text{-羟基-3-甲氧基苯亚甲基})\text{苯甲酰肼}(\mathbf{2}))$, 并通过物理化学方法和单晶 X-射线衍射表征了它们的结构。在每个配合物中, V 原子都采取八面体配位构型, 利用配体 L 中的 3 个给体原子和 1 个甲氧基配体的氧原子定义其赤道面, 利用 1 个酰肼氧原子和 1 个甲氧基氧原子占据其 2 个轴向位置。本文还研究了这 2 个配合物对幽门螺旋杆菌脲酶的抑制活性。在浓度为 $100 \mu\text{mol} \cdot \text{L}^{-1}$ 时, 配合物 **1** 和 **2** 对脲酶的抑制率分别为 $(82.0\% \pm 2.8\%)$ 和 $(28.2\% \pm 1.7\%)$ 。此外, 还做了配合物和幽门螺旋杆菌脲酶的分子对接研究。

关键词: 酰肼; 钒氧(V)配合物; 晶体结构; 脲酶; 抑制剂

中图分类号: O614.51^{†1}

文献标识码: A

文章编号: 1001-4861(2012)09-1959-08

Synthesis, Structures, and Helicobacter Pylori Urease Inhibition of Oxovanadium(V) Complexes with Hydrazones

ZHANG Ji-Cai LI Hai-Hua XIAN Dong-Mei ZHANG Mei

ZHEN Miao-Miao ZHAO Yue YOU Zhong-Lu*

(Department of Chemistry and Chemical Engineering, Liaoning Normal University, Dalian, Liaoning 116029, China)

Abstract: Two new structural similar oxovanadium(V) complexes with the formulae $[\text{VOL}(\text{OCH}_3)(\text{CH}_3\text{OH})](\text{L}=\text{L}^1=2\text{-chloro-}N'-(5\text{-chloro-2-hydroxybenzylidene})\text{benzohydrazide}(\mathbf{1}); \text{L}=\text{L}^2=2\text{-chloro-}N'-(2\text{-hydroxy-3-methoxybenzylidene})\text{benzohydrazide}(\mathbf{2}))$, have been synthesized and characterized by physico-chemical methods and single-crystal X-ray diffraction. The V atom in each complex is in an octahedral coordination, with the three donor atoms of L and one methanolato O atom defining the equatorial plane, and with one oxo O atom and one methanol O atom occupying the axial positions. The complexes were evaluated for their urease inhibitory activities. The percent inhibition of the complexes **1** and **2** at the concentration of $100 \mu\text{mol} \cdot \text{L}^{-1}$ on *Helicobacter pylori* urease are $82.0\% \pm 2.8\%$ and $28.2\% \pm 1.7\%$. The molecular docking study of the complexes with the urease was performed. CCDC: 844338, **1**; and 844339, **2**.

Key words: hydrazone; oxovanadium(V) complex; crystal structure; urease; inhibitor

Urease has important negative effects in human, stockbreeding, and agriculture^[1-3]. Control of the activity of urease through the use of inhibitors could counteract these negative effects. The metal complexes have been proved to be a kind of versatile enzyme inhibitors^[4].

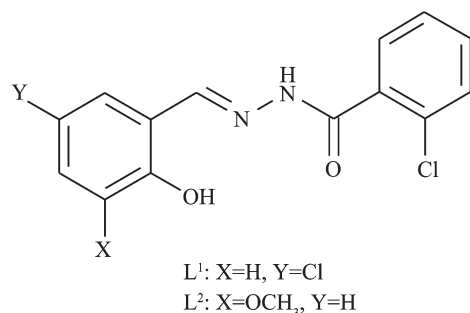
Among the versatile metal complexes, those derived from hydrazones have received particular attention in biological and medicinal chemistry^[5-7]. In recent years, the vanadium complexes have been reported to have interesting biological activities such as normalizing

收稿日期: 2012-03-01. 收修改稿日期: 2012-05-08.

国家自然科学基金(No.20901036), 辽宁省高校优秀青年人才支持计划(No.LJQ2011114)资助项目。

*通讯联系人。E-mail: youzhonglu@yahoo.com.cn

the high blood glucose levels and acting as models of haloperoxidases^[8-10]. It is notable that Ara and co-workers reported that the binuclear vanadium(IV) complexes possess interesting urease inhibitory activities^[11]. Aslam and co-workers reported that the Schiff bases with hydrazone type also possess urease inhibitory activities^[12]. In order to evaluate the urease inhibitory activities of the vanadium complexes with hydrazone ligands, in the present paper, two new oxovanadium(V) complexes with the formulae $[\text{VOL}(\text{OCH}_3)(\text{CH}_3\text{OH})]$ ($\text{L} = \text{L}^1 = 2\text{-chloro-}N'-(5\text{-chloro-2-hydroxybenzylidene})\text{benzohydrazide}$ (**1**); $\text{L} = \text{L}^2 = 2\text{-chloro-}N'-(2\text{-hydroxy-3-methoxybenzylidene})\text{benzohydrazide}$ (**2**); Scheme 1), have been synthesized and structurally characterized. The urease inhibitory activity and the molecular docking analysis of the complexes with *Helicobacter pylori* urease were investigated.



Scheme 1 The hydrazone ligands

1 Experimental

1.1 General methods and materials

Starting materials, reagents and solvents were purchased from commercial suppliers and purified before use. Protease inhibitor (Complete Mini EDTA-free) was purchased from Roche Diagnostics GmbH (Mannheim, Germany) and brucella broth was from Becton-Dickinson (Cockeysville, MD). Horse serum was obtained from Hyclone (Utah, America). Elemental analyses were performed on a Perkin-Elmer 240C elemental analyzer. The IR spectra were recorded on a Jasco FT/IR-4000 spectrometer as KBr pellets in the $4\,000\sim 200\text{ cm}^{-1}$ region. Molar conductance was measured with a Shanghai DDS-11A conductometer. X-ray diffraction was carried out on a Bruker SMART 1000 CCD diffractometer.

1.2 Synthesis of the complexes

$[\text{VOL}^1(\text{OCH}_3)(\text{CH}_3\text{OH})]$ (**1**): 5-Chlorosalicylaldehyde (0.156 g, 1 mmol) and 2-chlorobenzohydrazide (0.171 g, 1 mmol) were mixed in methanol (30 mL). The mixture was stirred at ambient temperature for 30 min to give colorless solution. To the solution was added with stirring a methanolic solution (15 mL) of VO(acac)₂ (0.27 g, 1 mmol). The final mixture was further stirred for 30 min at ambient temperature to give a deep brown solution. Upon standing at room temperature, brown block-shaped crystals of **1**, suitable for X-ray crystal structural determination were formed. The crystals were isolated, washed three times with cold methanol and dried in air. Yield 63%. IR data (cm^{-1}): 3 214 (br, w), 1 606 (s), 1 542 (s), 1 507 (m), 1 474 (w), 1 463 (m), 1 474 (w), 1 379 (m), 1 348 (s), 1 278 (s), 1 195 (m), 1 146 (w), 1 092 (w), 1 050 (s), 1 019 (w), 973 (s), 949 (w), 912 (w), 882 (w), 823 (w), 775 (w), 743 (m), 669 (w), 636 (m), 593 (w), 573 (w), 501 (w), 486 (w), 452 (w), 425 (w), 406 (w), 349 (w). Anal. Calcd. for $\text{C}_{16}\text{H}_{15}\text{Cl}_2\text{N}_2\text{O}_3\text{V}$ (%): C, 44.0; H, 3.5; N, 6.4. Found(%): C, 43.7; H, 3.6; N, 6.5.

$[\text{VOL}^2(\text{OCH}_3)(\text{CH}_3\text{OH})]$ (**2**): The complex **2** was prepared and crystallized by the similar procedure as that described for **1**, with 5-chlorosalicylaldehyde replaced with 3-methoxysalicylaldehyde (0.152 g, 1 mmol). Yield 72%. IR data (cm^{-1}): 3 336 (br, w), 1 614 (s), 1 559 (s), 1 530 (m), 1 474 (m), 1 450 (m), 1 437 (m), 1 352 (m), 1 276 (m), 1 257 (s), 1 224 (w), 1 148 (w), 1 107 (w), 1 071 (m), 1 055 (m), 1 026 (w), 982 (m), 919 (w), 869 (w), 756 (w), 735 (m), 662 (w), 621 (m), 591 (w), 498 (w), 445 (w), 423 (w), 382 (w), 358 (w). Anal. Calcd. for $\text{C}_{17}\text{H}_{18}\text{ClN}_2\text{O}_6\text{V}$ (%): C, 47.2; H, 4.2; N, 6.5. Found(%): C, 47.1; H, 4.1; N, 6.5.

1.3 X-ray crystallography

Diffraction intensities for the complexes were collected at 298(2) K using a Bruker SMART 1000 CCD area-detector diffractometer with Mo $K\alpha$ radiation ($\lambda = 0.071\,073\text{ nm}$). The collected data were reduced with the SAINT program^[13], and multi-scan absorption correction was performed using the SADABS program^[14]. The structures were solved by direct method and refined against F^2 by full-matrix least-squares method

using the SHELXTL package^[15]. All of the non-hydrogen atoms were refined anisotropically. The methanol H atoms in the complexes were located from difference Fourier maps and refined isotropically, with O-H distances restrained to 0.085(1) nm. The remaining hydrogen atoms were placed in calculated positions and constrained to ride on their parent atoms. The crystallographic data for the complexes are summarized in Table 1. Selected bond lengths and angles are given in Table 2. Crystallographic data for the complexes have been deposited with the Cambridge Crystallographic Data Centre.

CCDC: 844338, **1**; and 844339, **2**.

1.4 Urease inhibitory activity assay

Helicobacter pylori (ATCC 43504; American Type Culture Collection, Manassas, VA) was grown in brucella broth supplemented with 10% heat-inactivated horse serum for 24 h at 37 °C under microaerobic condition (5% O₂, 10% CO₂, and 85% N₂). The method of preparation of *Helicobacter pylori* urease by Mao^[16] was followed. Briefly, broth cultures (50 mL, 2.0×10⁸ CFU·mL⁻¹) were centrifuged (5 000 g, 4 °C) to collect the bacteria, and after washing twice with phosphate-buffered saline (pH 7.4), the *Helicobacter pylori* precipitation was stored at -80 °C. While the *Helicobacter pylori* was returned to room

Table 1 Crystal data for the complexes

Complex	1	2
Chemical Formula	C ₁₆ H ₁₅ Cl ₂ N ₂ O ₅ V	C ₁₇ H ₁₈ ClN ₂ O ₆ V
Formula weight	437.1	432.7
Crystal shape / colour	Block / brown	Block / brown
Crystal size / mm	0.27×0.23×0.22	0.17×0.13×0.13
<i>T</i> / K	298(2)	298(2)
λ (Mo <i>K</i> α) / nm	0.071 073	0.071 073
Crystal system	Monoclinic	Monoclinic
Space group	<i>C</i> 2/ <i>c</i>	<i>P</i> 2 ₁ / <i>c</i>
<i>a</i> / nm	2.749 7(3)	0.975 0(3)
<i>b</i> / nm	0.796 6(2)	1.955 3(7)
<i>c</i> / nm	2.018 5(2)	1.088 9(4)
β / (°)	122.925(2)	112.896(3)
<i>V</i> / nm ³	3.711 2(11)	1.912 3(11)
<i>Z</i>	8	4
μ (Mo <i>K</i> α) / cm ⁻¹	0.852	0.694
<i>T</i> _{min}	0.803	0.891
<i>T</i> _{max}	0.835	0.915
<i>D</i> _c / (g·cm ⁻³)	1.565	1.503
Reflections collected	10 223	11 881
Independent reflections	3 991	4 126
Observed reflections (<i>I</i> ≥ 2σ(<i>I</i>))	2 379	2 871
Parameters	240	250
Restraints	1	1
Goodness-of-fit on <i>F</i> ²	1.023	1.017
<i>R</i> _{int}	0.056 2	0.039 6
<i>R</i> ₁ (<i>I</i> ≥ 2σ(<i>I</i>))	0.051 5	0.047 5
<i>wR</i> ₂ (<i>I</i> ≥ 2σ(<i>I</i>))	0.107 7	0.100 7
<i>R</i> ₁ (all data)	0.098 8	0.075 8
<i>wR</i> ₂ (all data)	0.125 7	0.112 4

Table 2 Selected bond lengths (nm) and angles (°) for the complexes

1					
V1-O1	0.185 2(2)	V1-O2	0.194 7(2)	V1-O3	0.239 4(3)
V1-O4	0.175 7(2)	V1-O5	0.157 8(3)	V1-N1	0.212 8(3)
O5-V1-O4	103.3(1)	O5-V1-O1	100.1(1)	O4-V1-O1	101.8(1)
O5-V1-O2	97.1(1)	O4-V1-O2	93.8(1)	O1-V1-O2	153.3(1)
O5-V1-N1	96.4(1)	O4-V1-N1	158.1(1)	O1-V1-N1	84.0(1)
O2-V1-N1	74.0(1)	O5-V1-O3	174.8(1)	O4-V1-O3	81.5(1)
O1-V1-O3	80.8(1)	O2-V1-O3	80.2(1)	N1-V1-O3	78.6(1)
2					
V1-O1	0.184 3(2)	V1-O3	0.196 4(2)	V1-O4	0.158 4(2)
V1-O5	0.232 1(2)	V1-O6	0.178 2(2)	V1-N1	0.211 5(2)
O4-V1-O6	101.5(1)	O4-V1-O1	100.8(1)	O6-V1-O1	102.0(1)
O4-V1-O3	96.0(1)	O6-V1-O3	94.0(1)	O1-V1-O3	153.8(1)
O4-V1-N1	96.4(1)	O6-V1-N1	159.8(1)	O1-V1-N1	83.6(1)
O3-V1-N1	74.7(1)	O4-V1-O5	175.8(1)	O6-V1-O5	82.3(1)
O1-V1-O5	80.0(1)	O3-V1-O5	81.9(1)	N1-V1-O5	79.6(1)

temperature, and mixed with 3 mL of distilled water and protease inhibitors, sonication was performed for 60 s. Following centrifugation (15 000 g, 4 °C), the supernatant was desalted through SephadexG-25 column (PD-10 columns, Amersham-Pharmacia Biotech, Uppsala, Sweden). The resultant crude urease solution was added to an equal volume of glycerol and stored at 4 °C until use in the experiment. The mixture, containing 25 µL (4U) of *Helicobacter pylori* urease and 25 µL of the test compound, was pre-incubated for 3 h at room temperature in a 96-well assay plate. Urease activity was determined by measuring ammonia production using the indophenol method as described by Weatherburn^[17].

1.5 Molecular docking study

Molecular docking of the complexes into the 3D X-ray structures of *Helicobacter pylori* urease structure (entry 1E9Y in the Protein Data Bank) was carried out by using the AutoDock 4.2 software as implemented through the graphical user interface AutoDockTools (ADT 1.5.4).

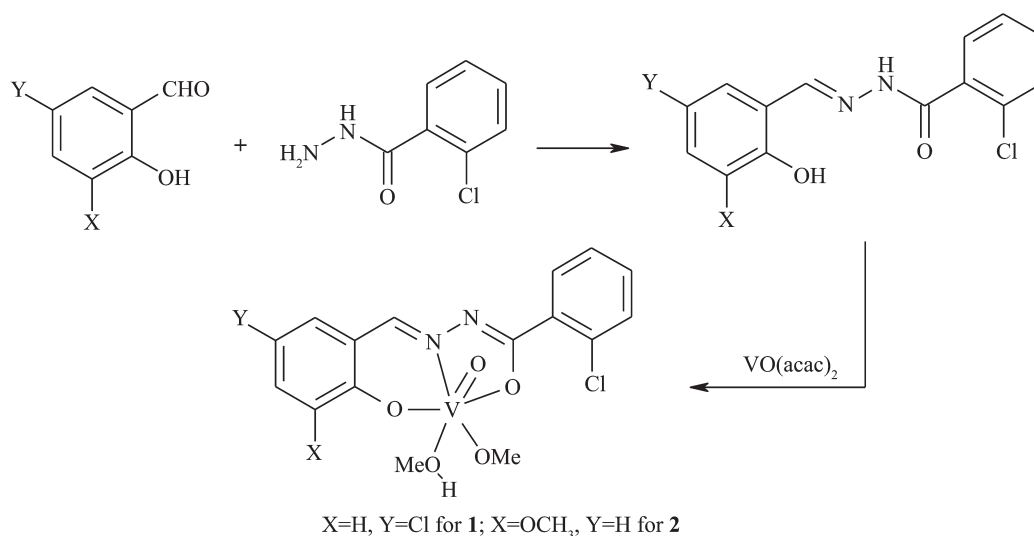
The graphical user interface AutoDockTools was employed to setup the enzymes: all hydrogens were added, Gasteiger charges were calculated and non-polar hydrogens were merged to carbon atoms. The Ni

initial parameters are set as $r=0.117$ nm, $q=+2.0$, and van der Waals well depth of 0.418 kJ·mol⁻¹^[18]. The AutoDockTools was used to generate the docking input files. In the docking grid box size of 7.0 nm \times 7.0 nm \times 6.0 nm for both complexes points in x , y , and z directions was built, the maps were centered on the original ligand molecule in the catalytic site of the protein. A grid spacing of 0.0375 nm and a distances-dependent function of the dielectric constant were used for the calculation of the energetic map. 100 runs were generated by using Lamarckian genetic algorithm searches. Default settings were used with an initial population of 50 randomly placed individuals, a maximum number of 2.5×10^6 energy evaluations, and a maximum number of 2.7×10^4 generations. A mutation rate of 0.02 and a crossover rate of 0.8 were chosen. The results of the most favorable free energy of binding were selected as the resultant complex structures.

2 Results and discussion

2.1 Chemistry

The hydrazone ligands were readily prepared by the condensation of 2-chlorobenzohydrazide with 5-chlorosalicylaldehyde and 3-methoxysalicylaldehyde,



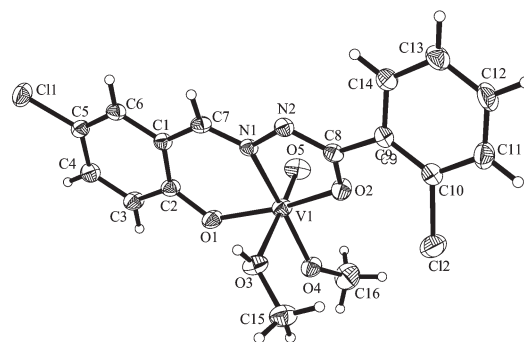
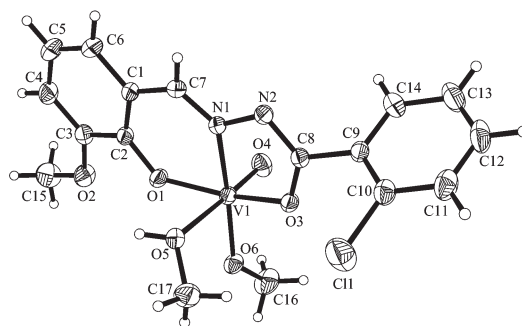
Scheme 2 The preparation of the complexes

respectively, in methanol at ambient condition. The hydrazones were not isolated and purified, which were further used to prepare the oxovanadium complexes with VO(acac)₂ (Scheme 2). The single crystals were obtained by slow evaporation of the methanolic solution of the complexes. All of the ligands and the complexes are stable in air at room temperature. The molar conductivity of the complexes measured in methanol at concentration of 10⁻³ mol·L⁻¹ are 18 Ω⁻¹·cm²·mol⁻¹ for **1** and 15 Ω⁻¹·cm²·mol⁻¹ for **2**, indicating the non-electrolytic nature of the complexes in solution^[19].

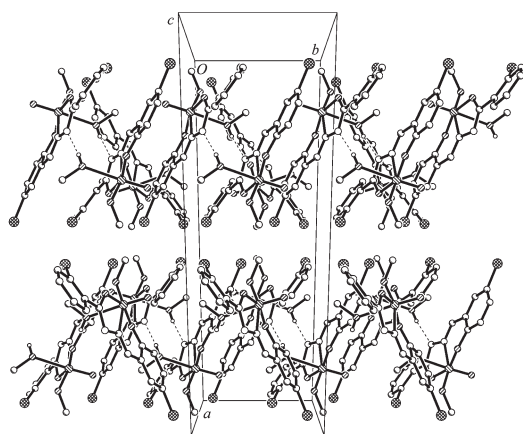
2.2 Structure description of the complexes

The molecular structures of the complexes **1** and **2** are shown in Fig.1 and 2, respectively. X-ray crystallography reveals that the complexes are structural similar oxovanadium(V) compounds, with slight difference between the hydrazone ligands. Each V atom in the complexes is in an octahedral coordination, with the three donor atoms of L and one methanolato O atom defining the equatorial plane, and with one oxo O atom and one methanol O atom occupying the axial positions. The distances between atoms V1 and O5 in **1**, and atoms V1 and O4 in **2** are in the range 0.157 8(3)~0.158 4(2) nm, indicating they are typical V=O bonds. The coordinate bond lengths in the complexes are comparable to each other, and also comparable to those observed in oxovanadium

complexes with octahedral coordination^[20-21]. The distortion of the octahedral coordination can be observed from the coordinate bond angles, ranging from 74.0(1)° to 103.3(1)° for **1**, and from 74.7(1)° to 102.0(1)° for **2**, for the perpendicular angles, and from 153.3 (1)° to 174.8(1)° for **1**, and from 153.8(1)° to 175.8(1)° for **2**, for the diagonal angles. The displacement of the V

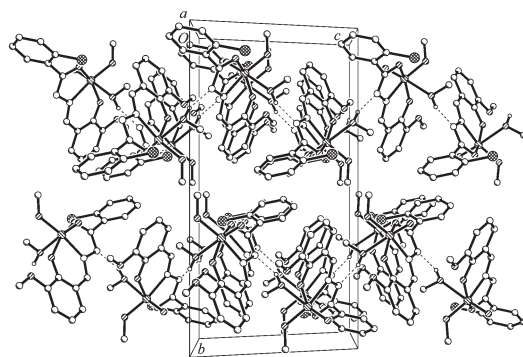
Fig.1 Molecular structure of **1** with displacement ellipsoids are drawn at 30% probability levelFig.2 Molecular structure of **2** with displacement ellipsoids are drawn at 30% probability level

atoms from the equatorial planes toward the axial oxo O atoms are 0.031 5(1) nm for **1**, and 0.029 8(1) nm for **2**. The formation of the coordinate bonds with the V atoms, together with the delocalization, lead to the planarity of the hydrazone ligands. The dihedral angles between the two substituted benzene rings are 65.1(2)° for **1**, and 13.2(2)° for **2**. In the crystal structures of the complexes, molecules are linked through intermolecular O—H···N hydrogen bonds, forming 1D chains, as shown in Fig.3 and 4.



Hydrogen bonds are shown as thin dashed lines

Fig.3 Molecular packing of **1** viewed along the *c* axis



Hydrogen bonds are shown as thin dashed lines

Fig.4 Molecular packing of **2** viewed along the *c* axis

2.3 Infrared spectra

The weak and broad absorptions centered at 3 214 cm⁻¹ for **1** and 3 336 cm⁻¹ for **2**, are assigned to the vibrations of the hydroxyl groups of the coordinate methanol molecules. The typical strong $\nu(\text{C}=\text{O})$ absorption bands and the sharp $\nu(\text{N}-\text{H})$ absorption bands of the free hydrazones are absent in the complexes, indicating the enolisation of the amide functionalities

and subsequent proton replacement by the V atoms. The strong absorption bands at 1 348 cm⁻¹ for **1** and 1 352 cm⁻¹ for **2** are assigned to the $\nu(\text{C}-\text{O})$ (enolic) vibrations. The strong absorption bands at 1 606 cm⁻¹ for **1** and 1 614 cm⁻¹ for **2** are assigned to the azomethine groups, $\nu(\text{C}=\text{N})$. The bands indicative of the V=O vibrations are at 912 cm⁻¹ for **1** and 919 cm⁻¹ for **2**. The close resemblance of the shape and the positions of the bands suggest similar coordination modes for the complexes, in accordance with the structural features.

2.4 Pharmacology

The results of the urease inhibition are summarized in Table 3. When compared with the reference inhibitor acetohydroxamic acid (AHA), the free hydrazones and the complex **2** have very weak interactions against the urease. It is interesting that complex **1** has effective activity with the percent inhibition of 82.0±2.7 (100 $\mu\text{mol}\cdot\text{L}^{-1}$), and with IC₅₀ value of (53.9±1.9) $\mu\text{mol}\cdot\text{L}^{-1}$, which is comparable to those of the AHA, and much better than the vanadyl sulfate with an IC₅₀ value of (207±3) $\mu\text{mol}\cdot\text{L}^{-1}$.

Table 3 Inhibition of urease by the tested materials

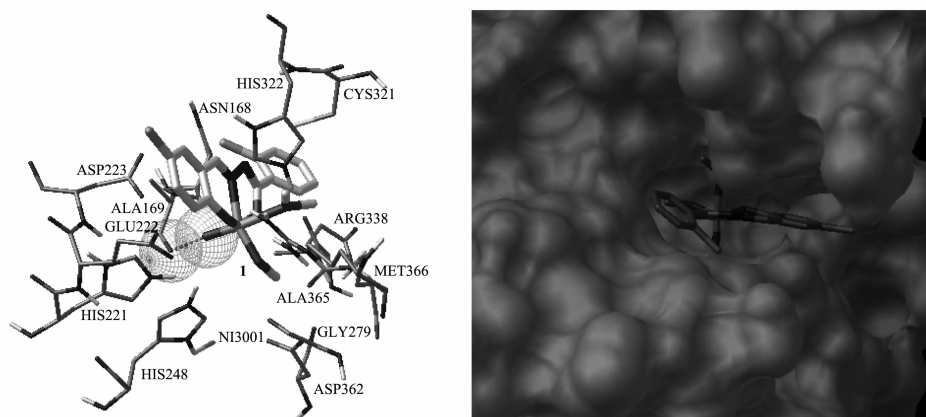
Tested materials	Percent inhibition	IC ₅₀ / ($\mu\text{mol}\cdot\text{L}^{-1}$)
1	82.0±2.7	53.9±1.9
2	28.1±1.8	—
H ₂ L ¹	18.2±1.5	—
H ₂ L ²	11.0±1.3	—
Vanadyl sulfate	22.3±2.7	207±3
Acetohydroxamic acid	89.3±3.2	42.0±2.5

Concentration of the tested material is 100 $\mu\text{mol}\cdot\text{L}^{-1}$

Considering that the difference of the structures is only the substituted groups of the benzene rings of the hydrazone ligands, viz. 5-Cl for **1** and 3-OCH₃ for **2**, it may conclude that the substitute groups of the hydrazone ligands can severely influence the urease inhibitory activities of the oxovanadium(V) complexes.

2.5 Molecular docking study

The molecular docking study was performed to investigate the binding effects between the complex **1** and the active sites of the *Helicobacter pylori* urease. In the X-ray structure available for the native *Helicobacter pylori* urease, the two nickel atoms were



Left: The interactions among the residues and the complex; Right: The enzyme is shown as Surface, and the complex is shown as sticks

Fig.5 Binding mode of **1** with *Helicobacter pylori* urease

coordinated by HIS136, HOS138, KCX219, HIS248, HIS274, ASP362 and water molecules, while in the AHA-inhibited urease, these water molecules were replaced by AHA^[22]. In order to give an explanation and understanding of the inhibitory activity of the complex **1**, molecular docking of the complex molecule into the AHA binding site of the urease was performed. The binding model of the complex with the urease was depicted in Fig.5. It can be seen that the molecule of **1** is well filled in the active pocket of the urease, and forms several short contacts with the residues of the active center. However, the molecule of **2** is located at the entry of the pocket, which is relatively far away from the active center. The docking energy of the complexes with the urease are $-27.55 \text{ kJ} \cdot \text{mol}^{-1}$ for **1** and $-13.67 \text{ kJ} \cdot \text{mol}^{-1}$ for **2**. It is notable that the docking energy of **1** is much lower than that of the AHA ($-20.94 \text{ kJ} \cdot \text{mol}^{-1}$). The results of the molecular docking study could explain the effective inhibitory activity of **1** against *Helicobacter pylori* urease.

3 Conclusions

The present paper reports the synthesis and structures of two new oxovanadium(V) complexes with similar hydrazone ligands. The complexes were evaluated in vitro for their inhibitory activities against *Helicobacter pylori* urease. The chloro-substituted complex **1** shows effective inhibitory activity against the urease. Considering the vanadium complexes have interesting biological activities and have been widely

used in medicine, the complex **1** in this paper deserves further modify to improve the activity.

References:

- [1] Francisco S S, Urrutia O, Martin V, et al. *J. Sci. Food Agr.*, **2011**,**91**:1569-1575
- [2] Xiao Z P, Ma T W, Fu W C, et al. *Eur. J. Med. Chem.*, **2010**,**45**:5064-5070
- [3] Barros T G, Williamson J S, Antunes O A C, et al. *Lett. Drug Des. Discovery*, **2009**,**6**:186-192
- [4] Louie A Y, Meade T J. *Chem. Rev.*, **1999**,**99**:2711-2734
- [5] Bernhardt P V, Chin P, Sharpe P C, et al. *Dalton Trans.*, **2007**,**30**:3232-3244
- [6] Bernhardt P V, Wilson G J, Sharpe P C, et al. *J. Biol. Inorg. Chem.*, **2008**,**13**:107-119
- [7] Yaul A R, Dhande V V, Suryawanshi N J, et al. *Polish J. Chem.*, **2009**,**83**:565-571
- [8] Willsky G R, Goldfine A B, Kostyniak P J, et al. *J. Inorg. Biochem.*, **2001**,**85**:33-42
- [9] Orvig C, Caravan P, Gelmini L, et al. *J. Am. Chem. Soc.*, **1995**,**117**:12759-12770
- [10] Messerschmidt A, Prade L, Wever R. *Biol. Chem.*, **1997**, **378**:309-315
- [11] Ara R, Ashiq U, Mahroof-Tahir M, et al. *Chem. Biodivers.*, **2007**,**4**:58-71
- [12] Aslam M A S, Mahmood S, Shahid M, et al. *Eur. J. Med. Chem.*, **2011**,**46**:5473-5479
- [13] Bruker, SMART and SAINT, Bruker AXS Inc, Madison, **2002**.
- [14] Sheldrick G M. SADABS, University of Göttingen, Germany, **1996**.
- [15] Sheldrick G M. SHELXTL V5.1, Software Reference Manual,

- Bruker AXS Inc, Madison, **1997**.
- [16]Mao W J, Lü P C, Shi L, et al. *Bioorg. Med. Chem.*, **2009**, **17**:7531-7536
- [17]Weatherburn M W. *Anal. Chem.*, **1967**,**39**:971-974
- [18]Krajewska B, Zaborska W. *Bioorg. Chem.*, **2007**,**35**:355-365
- [19]Geary W J. *Coord. Chem. Rev.*, **1971**,**7**:81-122
- [20]LIU Jiu-Hui(刘九辉), WU Xiao-Yuan(吴小园), ZHANG Quan-Zheng(张全争), et al. *Chinese J. Inorg. Chem.(Wuji Huaxue Xuebao)*, **2006**,**22**(6):1028-1032
- [21]DENG Zhao-Peng(邓兆鹏), GAO Shan(高山), ZHAO Hui(赵辉), et al. *Chinese J. Inorg. Chem.(Wuji Huaxue Xuebao)*, **2007**,**23**(1):173-176
- [22]Xiao Z P, Ma T W, Fu W C, et al. *Eur. J. Med. Chem.*, **2010**,**45**:5064-5070